COMMUNICATION

ChemComm
www.rsc.org/chemcomm

Nanotubes of poly(phenylene vinylene) derivative at the air/water interface†

Lin Guo,* Zhongkui Wu and Yingqiu Liang*

Key Lab of Mesoscopic Chemistry, Ministry of Education, Department of Chemistry, Nanjing University, Nanjing 210093, People's Republic of China. E-mail: linguo@nju.edu.cn; yqliang@nju.edu.cn; Fax: +86-25- 83317761; Tel: +86-25-83592369

Received (in Cambridge, UK) 16th March 2004, Accepted 12th May 2004
First published as an Advance Article on the web 11th June 2004

Different sizes of nanotubes of poly(2-methoxy-5-(*n*-hexadecyloxy)-*p*-phenylene vinylene) (MH-PPV) have been fabricated at the air/water interface by compressing a monolayer of MH-PPV beyond its collapse point, and their structural characteristics were studied by means of TEM, AFM, SAXRD, IRRAS.

Poly(*p*-phenylenevinylene) (PPV) is a conducting polymer which is known to exhibit electroluminescence (EL)[1] and nonlinear optical properties.[2] Preparation of conducting polymers in nanotube or nanowire shapes can provide us with conducting materials that can find a wide range of applications in nanoelectronic devices such as light emitting diodes,[3] photovoltaic devices,[4] sensors,[5] *etc*. Since the electronic and optical properties of the polymer films and nanostructures are inherently related to their local structure, it is vitally important to achieve great control of the self-assembly process that takes the polymer from the disordered state in solution into a well-ordered solid state.[6,7] Usually, thin films or fibers of PPV are prepared by soluble precursor routes.[8,9] However, large amounts of solvent and side products have to be removed during this process, which is expected to generate many defects such as bubbles in the final objects and to leave impurities from the solvent. Recently, PPV[10] and polythiophenyl[11] in the shapes of nanorods and nanotubes were successfully prepared by chemical vacuum deposition or electrochemical polymerizing method. However, there are no reports concerning the self-assembly of PPV nanotubes at the air/water interface. Herein, we report on a new approach to well-ordered poly(2-methoxy-5-(*n*-hexadecyloxy)-*p*-phenylene vinylene) (MH-PPV) nanotubes at the air/water interface by Langmuir–Blodgett (LB) techniques, and study their microstructure properties.

MH-PPV has been synthesized and characterized as previously reported.[7] It is known that MH-PPV can form densely packed monolayers with a π system plane perpendicular to the air/water interface and arrange in a π-stacked rigid crystalline structure.[7] As described below, MH-PPV monolayers spontaneously form tube-like structures when compressed beyond the collapse point at the air/water interface. Transmission electron micrograph (TEM) images of the aggregating state of MH-PPV transferred on to a copper net by LB techniques beyond the collapse point of MH-PPV monolayers show that some MH-PPV nanotubes of different sizes and forms are distributed over the substrate. As shown in Fig. 1(a), no pinholes are observed in the nanotubes of MH-PPV within the detection limits of TEM. The wall thickness and diameter of the MH-PPV nanotube are estimated to be 20 ± 2 nm and 130 ± 20 nm respectively. The wall thickness is much larger than the thickness of MH-PPV monolayers (2.5 nm, by XRD),[7] and roughly corresponds to eight stacked monolayers. This behavior indicates that the MH-PPV multilayer rather than the monolayer forms the wall of the nanotube. In fact, larger nanotubes of MH-PPV with wall thickness of 40 ± 5 nm were also observed in this experiment (Fig. 1(b)). Fig. 1(c) shows that there is a ribbon-like plate of MH-PPV partly rolled into a tube structure; the thickness of the plate measured by TEM is estimated to be 20 ± 5 nm, which is corresponds to eight stacked monolayers. This image may represent the possible mechanism of formation of the nanotubes although not all of the MH-PPV in its collapsed state in the film looks like this. It suggests that MH-PPV monolayer film spontaneously folds into multilayer structures and then rolls into tube structures when compressed beyond the collapse point on the LB-trough. Atomic force microscopy (AFM) permits visualization of the size of the smallest structure in the surface of the tube. The AFM image shown in Fig. 1(d) reveals that the tube exhibits a length of 6 microns, width of 130 nm and height of 90 nm. The possible MH-PPV molecule packing during the formation of the nanotubes is shown in the top scheme of Fig. 2. As the MH-PPV can not be totally transferred to the substrate nor produce an ordered array after collapse at the air/water interface, we cannot obtain the conversion of the polymer into nanotubes in this experiment.

Fig. 2 shows the hysteresis experiment on MH-PPV monolayers at the air/water interface at different surface pressures. It can be seen that the compression results of monolayers up to 30 mN m^{-1} (Fig. 2(a)) in the second compression–expansion cycle are slightly different from the first cycle, indicating that the monolayer below the collapse point is reasonably stable at the air/water interface. However, the hysteresis experiment on MH-PPV monolayers performed with a maximum pressure of 54 mN m^{-1} (shown in Fig. 2(b)), which is beyond the collapse pressure of the monolayer,

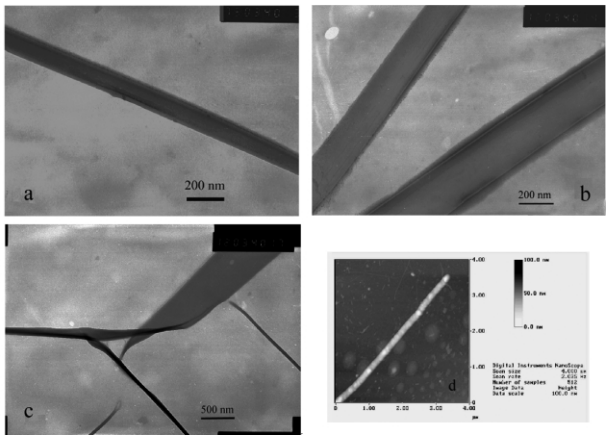

Fig. 1 a–c: TEM images of MH-PPV nanotubes at the collapse pressure of the MH-PPV monolayer. d: AFM images of MH-PPV nanotubes.

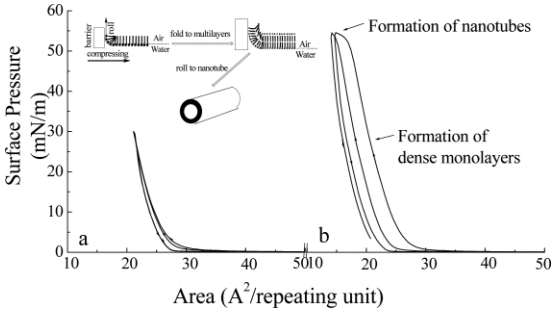

Fig. 2 Hysteresis isotherms of MH-PPV monolayers. a: maximum pressure set at 30 mN m^{-1}. b: maximum pressure set at 54 mN m^{-1} (beyond the collapse pressure). T = 293K; compression speed = 20 mm min^{-1}.

† Electronic supplementary information (ESI) available: Detailed experimental procedures and experimental conditions. See http://www.rsc.org/suppdata/cc/b4/b403870c/

DOI: 10.1039/b403870c

shows that the onset of the compression isotherm is shifted to 24.5 Å^2 and 23.5 Å^2 after completion the first and second compression–expansion cycles, respectively. Differences among the hysteresis cycles may be attributed to the formation of new aggregating states created by the reorganization of the film after the previous compression and expansion cycles.[6] It is clear that after collapse, a new aggregate of MH-PPV is formed at the air/water interface and the formation process is not reversible.

Fig. 3 shows the small-angle X-ray diffraction (SAXRD) pattern of the aggregated state of MH-PPV beyond the collapse point. There appears one sharp Bragg diffraction peak within the experimental region. Similar behavior can also be observed in the case of highly-ordered multilayers of the L-B film of MH-PPV transferred at a surface pressure of 30 mN m^{-1}.[7] This indicates that the aggregating state of MH-PPV beyond the collapse point is well ordered with a layer-by-layer structure. The interlayer spacing obtained from the Bragg diffraction peak is 116.9 Å; this value is more than two times as that of the L-B film of MH-PPV (49.9 Å).[7]

Fig. 4 shows the FT-IR reflection/absorption spectroscopy (IRRAS) of MH-PPV monolayers at the air/water interface under different surface pressure conditions.‡ It can be seen from this figure that with the surface pressure increased from 0 to 30 mN m^{-1}, there shows a strong single band at 1467 cm^{-1} which is attributed to the CH_2 scissoring mode of long alkyl chains (δ (CH_2)) (see Fig. 4a), and the CH_2 asymmetric and symmetric stretching bands of MH-PPV are shifted from 2921 and 2851 cm^{-1} to 2918 and 2850 cm^{-1}, respectively (Fig. 4b). However, when the monolayer is compressed beyond the collapse point, the δ (CH_2) mode splits into two bands at 1472 and 1462 cm^{-1}, and the two bands at 2918 and 2850 cm^{-1} show no obvious change. It is well known that the CH_2 scissoring vibration mode δ (CH_2) will be used as a fingerprint of the crystal lattice of hydrocarbon chains.[12,13] A strong singlet δ (CH_2) band at 1467 cm^{-1} is indicative of triclinic subcell packing with one molecular per unit cell; the splitting of the δ (CH_2) mode is well known as representing an orthorhombic unit cell that contains two crystallographically independent hydrocarbon chains. This behavior indicates that when the film collapsed and rolled into nanotube structures, the crystal lattice of hydrocarbon chains of MH-PPV changed from triclinic subcell packing to orthorhombic-type packing. The bands appearing at 2918 and 2850 cm^{-1} are indicative of the highly ordered (*trans*-zigzag conformation) alkyl chains.[13–14]

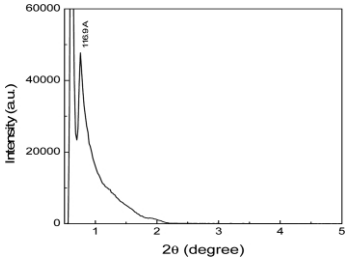

Fig. 3 Small-angle X-ray diffraction (SAXRD) pattern of the aggregated state of MH-PPV beyond the collapse point.

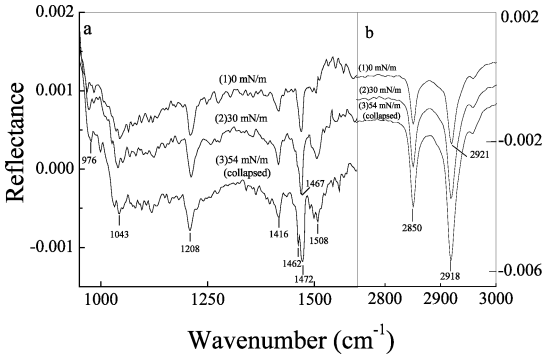

Fig. 4 IRRAS spectra of MH-PPV monolayers at the air/water interface under different surface pressure conditions at 293K. Spectra (1) to (3) are recorded at surface pressures of 0, 30 and 54 mN m^{-1} (collapse) respectively.

In conclusion, we have fabricated different sized nanotubes of MH-PPV at the air/water interfaces by compressing monolayers of MH-PPV beyond its collapse point, and studied the micro-structure of hydrocarbon chains of them for the first time. The diameter of the PPV tubes is on the nanoscale, which indicates their superior performance as light-emitting diodes and sensors. The fabrication is simple with no template-removing steps needed. The product is well ordered with a layer-by-layer structure; the crystal lattice of hydrocarbon chains of MH-PPV is changed from triclinic subcell packing to orthorhombic-type packing.

This work was financially supported by the Natural Science Foundation of Jiangsu Province and the National Natural Science Foundation of China (NSFC, NO. 20273029).

Notes and references

‡ Assignments of IR absorption bands of MH-PPV are: 2920 cm^{-1} (CH_3 asymmetric stretching), 2850 cm^{-1} (CH_2 stretch), 1508 cm^{-1} (semicircular phenyl stretch), 1467 cm^{-1}(δ (CH_2) scissors) 1406 cm^{-1} (semicircular phenyl stretch), 1208 cm^{-1} (phenyl–oxygen stretch), 1043 cm^{-1} (alkyl–oxygen stretch), 976 cm^{-1} (*trans* double bond CH wag).[6]

1 J. H. Burroughes, D. D. C. Bradley, A. R. Brown, R. N. Marks, K. Mackay, R. H. Friend, P. L. Burn and A. B. Holmes, *Nature*, 1990, **347**, 539.
2 J.-I. Jin and H.-K. Shim, in *Polymers for Second-order Nonlinear Optics*, ed. G. A. Lindsay and K. D. Singer, *ACS Symposium Series 601*, American Chemical Society, Washington DC, 1995, Ch. 17.
3 B. Bliznyuk, B. Ruhstaller, P. J. Brock, U. Scherf and S. A. Carter, *Adv. Mater.*, 1999, **11**, 1257.
4 H. Ago, K. Petritsch, M. S. P. Shaffer, A. H. Windle and R. H. Friend, *Adv. Mater.*, 1999, **11**, 1281.
5 J. Kong, N. R. Franklin, C. Zhou, M. G. Chapline, S. Peng, K. Cho and H. Dai, *Science*, 2000, **287**, 622.
6 J. G. Hagting, R. E. T. P. de Vos, K. Sinkovics, E. J. Vorenkamp and A. J. Schouten, *Macromolecules*, 1999, **32**, 3930.
7 Z. K. Wu, S. X. Wu and Y. Q. Liang, *Langmuir*, 2001, **17**, 7267.
8 R. A. Wessling, *J. Polym. Sci.: Polym. Symp.*, 1985, **72**, 55.
9 F. R. III. Denton and P. M. Lahti, in *Electrical and Optical Polymer Systems – Fundamentals, Methods, and Applications*, ed. D. L. Wise, Marcel Dekker, New York, 1998, Ch. 3.
10 K. Kim and J.-I. Jin, *Nano Lett.*, 2001, **1**, 631.
11 M. X. Fu, Y. F. Zhu, R. Q. Tan and G. Q. Shi, *Adv. Mater.*, 2001, **13**, 1874.
12 J. G. Weers and D. R. Scheuing, In *Fourier Transfer Infrared Spectroscopy in Colloid and Interface Science*, ed. D. R. Scheuing, American Chemical Society, Boston, 1991, p. 91.
13 J. Simon-Kutscher, A. Gericke and H. Hühnerfuss, *Langmuir*, 1996, **12**, 1027.
14 Y. Tian, *J. Phys. Chem.*, 1991, **95**, 9985.